CHARACTERIZATION OF THE RADIATION FIELD IN THE FCC-HH DETECTOR

M. I. Besana*, F. Cerutti, A. Ferrari, W. Riegler, V. Vlachoudis, CERN, Geneva, Switzerland

Abstract

As part of the post-LHC high-energy program, a study is ongoing to design a new 100 km long hadron collider, which is expected to operate at a centre-of-mass energy of 100 TeV and to accumulate up to 30 ab^{-1}, with a peak instantaneous luminosity that could reach 30 $10^{34}cm^{-2}s^{-1}$.

In this context, the evaluation of the radiation load on the detector is a key step for the choice of materials and technologies. In this contribution, a first detector concept will be presented. At the same time, fluence distributions, relevant for detector occupancy, and accumulated damage on materials and electronics will be shown. The effectiveness of a possible shielding configuration, intended to minimise the background in the muon chambers and tracking stations, will be presented.

INTRODUCTION

The radiation load at the Future Circular Collider (FCC-hh) [1] will be more challenging than at the LHC, since collision energy will be more than seven times higher and the foreseen ultimate instantaneous luminosity is 30 times higher. It is important also to evaluate the long term damage, since the integrated luminosity goal exceeds by two orders of magnitude the LHC one and by one order of magnitude the High Luminosity LHC (HL-LHC) one.

To this purpose, Monte Carlo simulations have been performed with FLUKA [2] using DPMJET-III [3] as proton proton collision generator. The non-elastic cross section at 100 TeV is assumed to be 108 mbarn. The radiation on the detector has been evaluated in terms of fluence rates to estimate the tracker occupancy for 30 $10^{34}cm^{-2}s^{-1}$. The long term damage has been assessed in terms of 1 MeV neutron equivalent fluence for displacement damage and of dose, for an integrated luminosity of 30 ab^{-1}. Only half of the detector has been implemented with FLUKA, but the contribution coming from the other half is accounted for. The impact of the backscattering from the Target Absorber Secondaries (TAS), the protection element in front of the final focus triplet, has not been included in this calculation, since, according to the current design of the interaction region [4], the absorber is expected to be outside the experimental cavern and therefore adequately shielded.

Detector Geometry

To fully exploit the potential of the machine, the detectors should have large $|\eta|$[1] acceptance. In fact, the Higgs boson will be generally produced with a high boost in the forward region, because its mass is significantly lower than the available energy at the collision. Figure 1 shows the first concept for a possible FCC-hh detector, which is composed of a central part cylindrically symmetric, similar to present ATLAS [5] and CMS [6] detectors, and a forward part, similar to LHCb detector [7]. The central part is characterised by the presence of a solenoid field, generated by a coil with a large radius of 6.25 m. A shielding coil is used to contain field lines. A dipole is foreseen in the forward region on both sides to enable the measurement of the high $|\eta|$ particles momentum.

Central Region Closest to the beam pipe is the Tracker, which will have the function of reconstructing the trajectory of the charged particles and it is designed to reach a 10% resolution on the transverse momentum (p_T) measurements for particles with p_T up to 10 TeV. It is composed of different silicon detectors and it extends from a radial distance from the beam axis (R) of 2.5 cm, where the first pixel layer is expected to be put, up to 2.5 m. Its length along the beam axis (z) is 16 m, centred around the interaction point. The whole system is enclosed by the Electromagnetic Calorimeter (EM-calo), which extends up R = 3.6 m and it is designed to precisely measure the energy of electrons and photons. It is based on a Liquid Argon technology, similar to the one used in ATLAS. Outside the EM-calo there is the Hadronic Calorimeter (HAD-calo), which extends up to 6 m and will measure the energy of hadronic particles. It is expected to be based on a scintillator technology and in the present design it is made by a mixture of iron and plastic. The whole calorimeter system has been designed to contain the generated showers and it has therefore a thickness which reaches 12 interaction lengths for hadrons. The solenoid coil extends from R = 6.25 m to R = 7.825 m, while the shielding solenoid is between R = 13 m and R = 13.475 m. The space between the two coils will be used for the Muon Spectrometer.

End-cap Region The calorimeter system has been designed to be hermetic up to $|\eta|$= 2.5. The end-cap calorimeters extend from z = 8 m to z = 11.5 m. The EM-calo has a thickness of 1.1 m, while the HAD-calo is 2.4 m thick. Muon chambers are put between 11.5 m and 14.8 m to measure the transverse momentum of muons up to $|\eta|$= 2.5.

Forward Region The forward region is designed to catch particles up to $|\eta| = 6$. On each side of the central detector, a dipole is put between z = 14.8 m and z = 21 m. These dipoles have lateral coils to counteract the forces between the solenoid and each dipole. Tracking stations are foreseen before and after the dipole region, to measure the

* maria.ilaria.besana@cern.ch

[1] $\eta \equiv -\ln\left[\tan\left(\frac{\theta}{2}\right)\right]$, where θ is the angle between the particle three-momentum **p** and the positive direction of the beam axis.

ISBN 978-3-95450-147-2

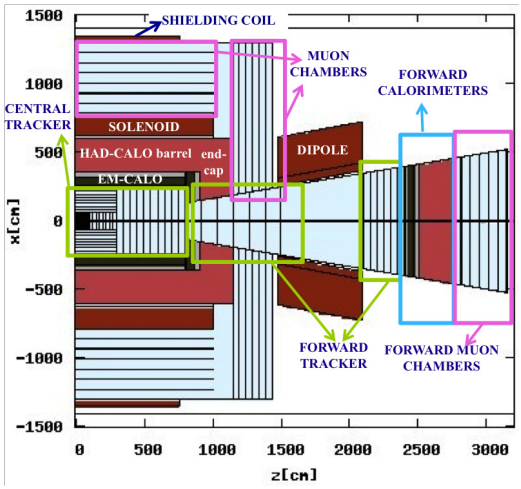

Figure 1: Detector layout: z-x view. The x axis is on the horizontal plane, pointing outside the ring; y axis is opposite to gravity and z axis is along the beam. The origin of the coordinate system corresponds to the nominal collision point. A detailed description is reported in the text.

angular deviation due to the dipole magnetic field. There are not tracking stations in the dipole region, since it is easier to build and maintain detectors outside and in order to avoid occupancy from loopers. After the Forward Tracker, calorimeters (Forward EM-calo and Forward HAD-calo) are foreseen between z = 24 m and z = 27.5 m. In the present model the same material composition of the barrel calorimeters is used. Radiation calculations have shown that fluence rates are significantly higher in this region and therefore a dedicated technology for these sub-detectors will be needed. Finally a Muon Spectrometer is put after the Forward HAD-calo, up to z = 31.5 m.

Magnetic Field The magnetic field is given by the superimposition of a solenoid field directed along the z axis and a dipole field along the y axis. As a result, the field in the dipole zone has not only a y-component and there is an up/down asymmetry: for positive y the values of the field are higher, as it can be seen in Fig. 2.

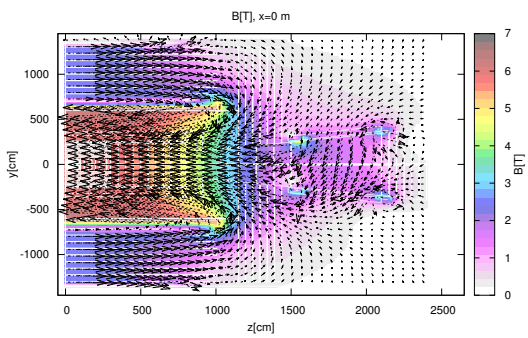

Figure 2: Magnetic field map: z-y view for x = 0 [8].

RADIATION CALCULATIONS

Charged Particles Fluence Rates

Fluence rates are shown in Fig. 3 on the z-x plane at y=0 and in Fig. 4 on the z-y plane at x=0. There is a significant dependence on R, but a week dependence on z: as expected, equi-fluence lines are substantially parallel to the z axis. In the first pixel layer, at R = 2.5 cm, the charged particle fluence rate is $2\,10^{10}$ Hz cm^{-2}. Particles are then absorbed by the barrel calorimeter and the fluence rate values go down by several orders of magnitude. On the other hand, a very significant generation area is represented by the forward calorimeters, where the fluence rate reaches 10^{11} Hz cm^{-2}. From there, particles repopulate back the Muon Spectrometer. The fluence rates are $2\,10^{5}$ Hz cm^{-2} and 10^{6} Hz cm^{-2} in the barrel and end-cap muon chambers respectively. These values are too high for a good muon identification and need to be reduced. As will be shown later in the paper, this can be achieved thanks to a shielding around the forward calorimeter. The distribution of charged particles is broader in the z-x plane because of the effect of the dipole field directed along the y-axis. The latter is also visible in the z-y plane, where the higher fluence rate red line at y>0 between 14 m and 17 m is due to electrons and positrons spiralling around magnetic field lines.

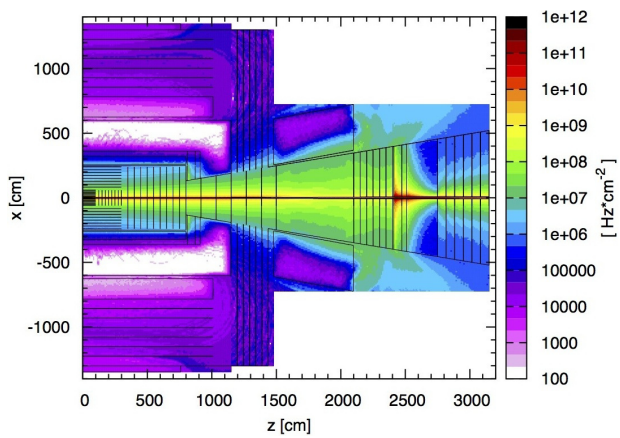

Figure 3: Charged particle fluence rate: z-x view. In the central region (z < 10.5 m) values are azimuthally averaged over 40 degrees around 0 (positive x) and π (negative x). In the forward region an average in the vertical direction around y=0 is done on a bin of 1 cm up to |x|=0.6 m and on a 10 cm bin for larger |x| values.

Long Term Damage

The long term damage has been quantified in terms of 1 MeV neutron equivalent fluence and of dose.

In the central region, at a radial distance below 50 cm, neutron fluence values exceed the ones expected at HL-LHC [9] (10^{16} cm^{-2}) by almost two orders of magnitude (we obtain $8\,10^{17}$ cm^{-2} at the first pixel layer), representing a technology challenge. On the external side of the barrel HAD-calo, neutron fluence is reduced down to 10^{10} cm^{-2}, while at the

ISBN 978-3-95450-147-2

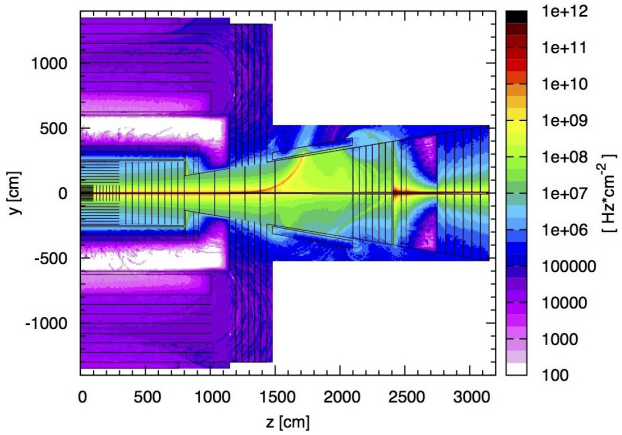

Figure 4: Charged particle fluence rate: z-y view. In the central region (z < 10.5 m) values are azimuthally averaged over 20 degrees around $\frac{\pi}{2}$ (positive y) and $-\frac{\pi}{2}$ (negative y). In the forward region an average in the horizontal direction around x=0 is done on a bin of 1 cm up to |y|=0.6 m and on a 10 cm bin for larger |y| values.

forward calorimeters it reaches 7 10^{18} cm^{-2}. These neutrons impact on the forward tracking stations and repopulate muon chambers. The neutron fluence on the tracking station closest to the Forward EM-calo is 10^{17} cm^{-2} at R = 50 cm and it goes below 10^{16} cm^{-2} for R > 2.5 m. In the muon chambers it reaches 10^{14} cm^{-2} in the barrel and 3 10^{15} cm^{-2} in the end-cap. These values are too high, but they can be mitigated with a shielding.

The dose in the first pixel layer is 600 MGy, while it is 10 GGy in the forward EM-calo. The maximum value in the end cap hadronic calorimeter is 0.4 MGy, which is excessive for a scintillator technology. A possible solution is to have an extended barrel HAD-calo up to z = 11.5 m with a radius larger than 3.6 m, where the dose is 2 kGy; the dose on the non-IP face of the HAD-calo at 3.6 m reaches 10 kGy, but it can be mitigated with a shielding. A Liquid Argon technology could be used for the end-cap HAD-calo for R < 3.6 m.

SHIELDING DESIGN AND EFFECTIVENESS

A shielding has been designed to be put in front of the forward calorimeters in order to protect the Forward Tracker. It is made by 5 cm of lithiated polyethylene, with a 2 mm thick cover of aluminium on the two sides. This material is used, since the neutron capture is mostly done without gamma emission, thanks to lithium. This shielding reduces the 1 MeV neutron equivalent fluence on the close by tracking layers by a factor of three.

Moreover, a massive shielding has to be put around the forward calorimeter up to the cavern wall, in order to protect the barrel and end-cap muon chambers from backscattered particles. Without shielding, the neutron fluence rate reaches 10^8 Hz cm^{-2}, causing a fake muon signal rate of the order of 100 kHz cm^{-2}. An analogous background level would be added by photons. The shielding is composed by a 2 m thick iron wall to remove high energy particles. A 5 cm thick layer of lithiated polyethylene is put externally to further slow down and capture neutrons. A 1 cm thick layer of lead is added as outer boundary, in order to absorb the rarely emitted photons. Figure 5 shows the effect of the shielding on the neutron fluence rate, which is reduced to 2 kHz cm^{-2} and to 10 kHz cm^{-2} in the barrel and end-cap muon chambers respectively, corresponding to a fake muon signal rate one thousand times lower. Photon fluence rate in those locations is at the level of 1 kHz cm^{-2} and it is expected to yield a fake muon signal of the order of 10 Hz cm^{-2}. These values are comparable to the rates that can be afforded with present technologies.

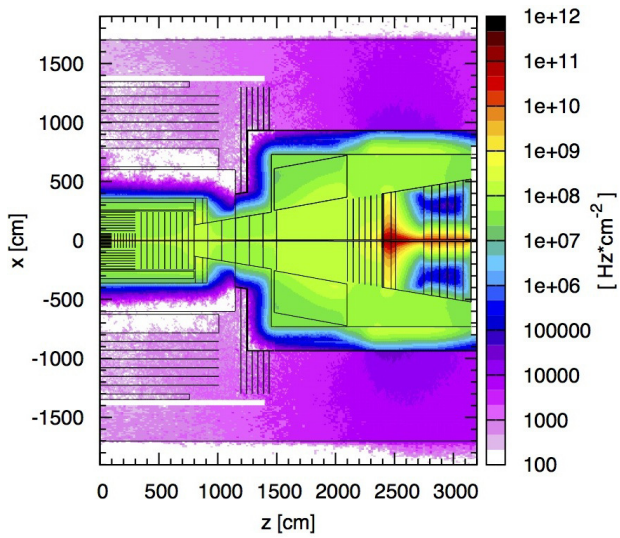

Figure 5: Neutron fluence rate in the presence of the shielding described in the text: z-x view.

CONCLUSION

A first concept of the detector has been implemented in FLUKA and the radiation load has been assessed in terms of fluence rates and long term damage. Based on these results, two different shielding systems have been conceived to protect forward tracking stations, muon chambers and electronics. The resulting mitigation is effective, leaving with values that are challenging, but manageable.

In the future, the detector design will be further optimised to find the best compromise between cost and performance. Alternative designs are under study, which for example don't foresee the presence of forward dipoles. It would be important to repeat the calculation for the new designs to highlight the effect of these changes in terms of radiation load.

ACKNOWLEDGMENT

This work has profited form useful discussions within the FCC-hh Machine Detector Interface and FCC-hh Detector working groups.

REFERENCES

[1] D. Schulte, "Preliminary collider baseline parameters", EuroCirCol-D1-1, 2015g.

[2] A. Ferrari, P.R. Sala, A. Fassò, and J. Ranft, "FLUKA: a multi-particle transport code", Rep. CERN-2005-10, INFN/TC 05/11, SLAC-R-773, Oct. 2005.

G. Battistoni *et al.*, "Overview of the FLUKA code", *Annals of Nuclear Energy*, vol. 82, pp. 10-18, Aug. 2015.

[3] S. Roesler, R. Engel, and J. Ranft, "The Monte Carlo event generator DPMJET-III", in *Proc. Monte Carlo 2000 Conference*, Lisbon, Portugal, Oct. 2000, A. Kling, F. Barao, M. Nakagawa, L. Tavora, P. Vaz eds., Springer-Verlag Berlin, pp. 1033-1038, 2001.

A. Fedynitch and R. Engel, "Revision of the high energy hadronic interaction models PHOJET/DPMJETIII", in *Proc. 14th International Conference on Nuclear Reaction Mechanisms*, Varenna, Italy, Jun. 2015 edited by F. Cerutti, M. Chadwick, A. Ferrari, T. Kawano and P. Schoofs, CERN Proceedings-2015-001 (CERN, Geneva, 2015), pp. 291-299, https://cds.cern.ch/record/2114737.

[4] M. I. Besana, F. Cerutti, S. Fartoukh, R. Martin, and R. Tomas, "Assessment and mitigation of the proton-proton collision debris impact on the FCC triplet", presented at the 7th Int. Particle Accelerator Conf. (IPAC'16), Busan, Korea, May 2016, paper TUPMW004.

[5] ATLAS Collaboration (G. Aad *et al.*), "The ATLAS Experiment at the CERN Large Hadron Collider", *Journal of Instrumentation*, vol. 3, S08003, Aug. 2008.

[6] CMS Collaboration (S. Chatrchyan *et al.*), "The CMS experiment at the CERN LHC", *Journal of Instrumentation*, vol. 3, S08004, Aug. 2008.

[7] LHCb Collaboration (A. Augusto Alves Jr. *et al.*), "The LHCb Detector at the LHC", *Journal of Instrumentation*, vol. 3, S08005, Aug. 2008.

[8] M. Mentink and H. Ten Kate, private communication, Jun. 2015.

[9] ATLAS Collaboration (G. Aad *et al.*), "Letter of Intent for the Phase-II Upgrade of the ATLAS Experiment", Rep. CERN-LHCC-2012-022, LHCC-I-023, 2012.

ISBN 978-3-95450-147-2